Genome-wide analysis of signaling networks regulating fatty acid–induced gene expression and organelle biogenesis

Ramsey A. Saleem,[1] Barbara Knoblach,[2] Fred D. Mast,[2] Jennifer J. Smith,[1] John Boyle,[1] C. Melissa Dobson,[2] Rose Long-O'Donnell,[1] Richard A. Rachubinski,[2] and John D. Aitchison[1,2]

[1]Institute for Systems Biology, Seattle, WA 98103
[2]Department of Cell Biology, University of Alberta, Edmonton, Alberta T6G 2H7, Canada

Reversible phosphorylation is the most common posttranslational modification used in the regulation of cellular processes. This study of phosphatases and kinases required for peroxisome biogenesis is the first genome-wide analysis of phosphorylation events controlling organelle biogenesis. We evaluate signaling molecule deletion strains of the yeast *Saccharomyces cerevisiae* for presence of a green fluorescent protein chimera of peroxisomal thiolase, formation of peroxisomes, and peroxisome functionality. We find that distinct signaling networks involving glucose-mediated gene repression, derepression, oleate-mediated induction, and peroxisome formation promote stages of the biogenesis pathway. Additionally, separate classes of signaling proteins are responsible for the regulation of peroxisome number and size. These signaling networks specify the requirements of early and late events of peroxisome biogenesis. Among the numerous signaling proteins involved, Pho85p is exceptional, with functional involvements in both gene expression and peroxisome formation. Our study represents the first global study of signaling networks regulating the biogenesis of an organelle.

Introduction

Understanding complex cellular responses to external cues demands a comprehensive analysis of the molecular networks governing signaling, transcription, and morphology. Systems biology provides an unprecedented opportunity to investigate such complex dynamic networks and can enable a comprehensive understanding of all the components governing a response and the interplay among them. The peroxisome is an attractive organelle to study using the approaches of systems biology. Peroxisomes are rapidly affected in size, number, and protein composition by changes in nutrients available to the cell, are required for cell survival only under specific conditions, and are relatively poorly understood with regard to their function and biogenesis, although their dysfunction has been shown to cause a variety of fatal or debilitating human conditions.

In yeast, peroxisomes are induced to proliferate in the presence of fatty acids through a biogenic pathway initiated by signaling events and transcriptional modulation preceding the coordinated activities of ~30 peroxins, which are collectively responsible for organelle egression from the ER, matrix protein import, and peroxisome division. Peroxisome biogenesis is a sequential process, beginning with the insertion of the membrane protein Pex3p into subdomains of the ER (Hoepfner et al., 2005) and ending with matrix protein entry into peroxisomes (Erdmann and Schliebs, 2005; Leon et al., 2006) to obtain metabolically active organelles. Yeast cells restrict the β-oxidation of fatty acids to peroxisomes (Hiltunen et al., 2003), and functional peroxisomes are therefore indispensable for yeast growth on media containing fatty acids as the principal carbon source.

The mechanisms through which environmental cues are transduced into activation of the peroxisome biogenic pathway remain largely unknown. These mechanisms could regulate peroxisome biogenesis at the level of the transcriptional status of genes encoding peroxisomal proteins, the trafficking of proteins and lipids that are destined to become constituents of peroxisomes,

R.A. Saleem and B. Knoblach contributed equally to this paper.

Correspondence to John D. Aitchison: jaitchison@systemsbiology.org; or Richard A. Rachubinski: rick.rachubinski@ualberta.ca

Abbreviations used in this paper: GO, gene ontology; ORE, oleate-responsive elements.

The online version of this paper contains supplemental material.

The Journal of Cell Biology, Vol. 181, No. 2, April 21, 2008 281–292
http://www.jcb.org/cgi/doi/10.1083/jcb.200710009

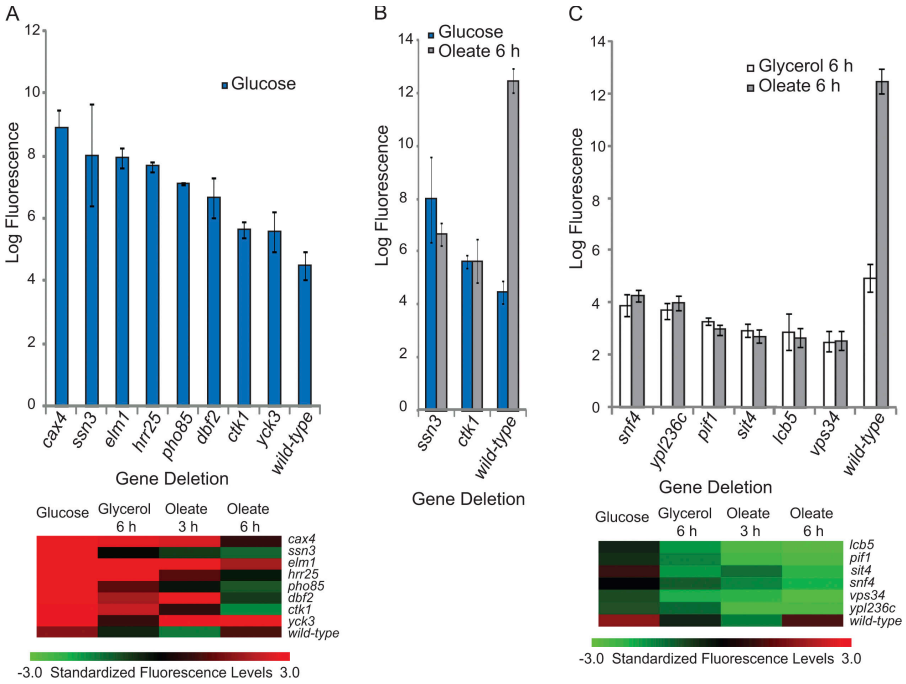

Figure 1. **Glucose repression.** (A) Pot1p-GFP levels in strains that are deleted for signaling molecules and that display an increase in Pot1p-GFP levels in glucose, which is indicative of a defect in glucose-mediated repression of the *POT1* locus. The y axis is shown on a $\log_{10}$ scale. (B) Plot of Pot1p-GFP fluorescence levels detected by FACS analysis of deletion strains with high levels of Pot1p-GFP in glucose but that exhibit a paucity of Pot1p-GFP after incubation in oleate-containing medium for 6 h. (C) A core of six signaling molecules whose deletion results in a severe defect in the ability of cells to express Pot1p-GFP in either glycerol or oleate after 6 h of incubation. These strains likely represent positive effectors of the transition from a glucose-repressed state to either a derepressed or oleate-induced state. The heat maps in A and C show the relative intensities of Pot1p-GFP fluorescence between mutants and wild-type cells in the four media conditions tested, with red and green indicating an increase and a decrease in fluorescence, respectively. Error bars show SD.

and/or the biological activities of proteins required for assembly, maturation, division, and turnover of peroxisomes. The proliferative capacity of peroxisomes coincides with the fatty acid–responsive transcriptional regulation of many of the genes encoding peroxisomal proteins (Karpichev and Small, 1998; Smith et al., 2002) and involves the transcriptional activators Adr1p, Oaf1p, and Pip2p (Rottensteiner et al., 1996; for review see Gurvitz and Rottensteiner, 2006). Oaf1p and Pip2p bind directly to oleate-responsive elements (OREs) in the promoter region of coordinately responsive peroxisomal matrix proteins (for review see Gurvitz and Rottensteiner, 2006). Adr1p is necessary for full ORE-mediated activation, as it directly activates *PIP2* and ORE-containing targets (Rottensteiner et al., 2003; Smith et al., 2007; for review see Gurvitz and Rottensteiner, 2006). Although Oaf1p appears to bind fatty acids directly, which in turn could directly activate this factor (Baumgartner et al., 1999; Phelps et al., 2006), the intracellular signaling networks that lead to the composite coordinated response resulting in the induction of peroxisomal proteins and the formation of the peroxisome itself are unknown.

Global transcriptome studies demonstrate that many peroxisomal matrix proteins respond coordinately to oleic acid (Koerkamp et al., 2002; Smith et al., 2002, 2007; for review see Gurvitz and Rottensteiner, 2006). We therefore used peroxisomal 3-ketoacyl-CoA thiolase (Pot1p), a peroxisomal matrix protein, as a prototype of peroxisomal matrix enzymes to query the effects of systematic deletions of signaling proteins in the yeast *Saccharomyces cerevisiae*. The *POT1* promoter exists predominantly in three states depending on the available carbon source (Einerhand et al., 1991; Igual et al., 1992). Glucose repression is dominant to both derepression and induction (Einerhand et al., 1991; Igual et al., 1992). Addition of oleate in the presence of glucose does not lead to the expression of genes encoding peroxisomal proteins. The second state is derepression. In the derepressed state, the promoter is no longer repressed by the presence of glucose but is also not induced by the removal of glucose. The third state is an induced state in which an ORE is bound by the transcription factors Oaf1p and Pip2p in response to fatty acid stimulation. The range of activation of the *POT1* promoter is over 1,000-fold, making this promoter comparable to the most strongly regulated promoters (Navarro and Igual, 1994). In the repressed state, the *POT1* promoter is expressed at only ~0.4% of the level of its induced state. In the derepressed state, the expression level is 14% (Einerhand et al., 1991). Similar condition-specific differences in the levels of the *POT1* gene product are seen by Northern and Western analyses. A genome-wide analysis of loss-of-function kinase and phosphatase mutant strains of *S. cerevisiae* allowed us the opportunity to assess the contributions made by individual kinases and phosphatases to the induction of oleate-responsive genes, such as *POT1*, and to peroxisome biogenesis. To identify signaling networks that are responsible for glucose derepression, oleate induction, and peroxisome biogenesis, we measured the expression of a peroxisomal reporter chimera, Pot1p-GFP, and the organellar biogenic response in signaling gene-deletion mutants grown in glucose, glycerol, and oleate. This study represents the first comprehensive investigation of kinase and phosphatase activity in the complex biological process of organelle biogenesis.

Results

A collection of 249 kinase and phosphatase gene deletion strains of *S. cerevisiae* expressing a chromosomally integrated gene fusion encoding Pot1p and GFP was evaluated for the expression of the chimera and the formation and functionality of peroxisomes. We addressed four parameters with respect to these processes: glucose repression, glycerol-mediated derepression, oleate induction, and peroxisome morphology. By incubating each signaling molecule deletion strain in glucose-, glycerol-, or oleate-containing

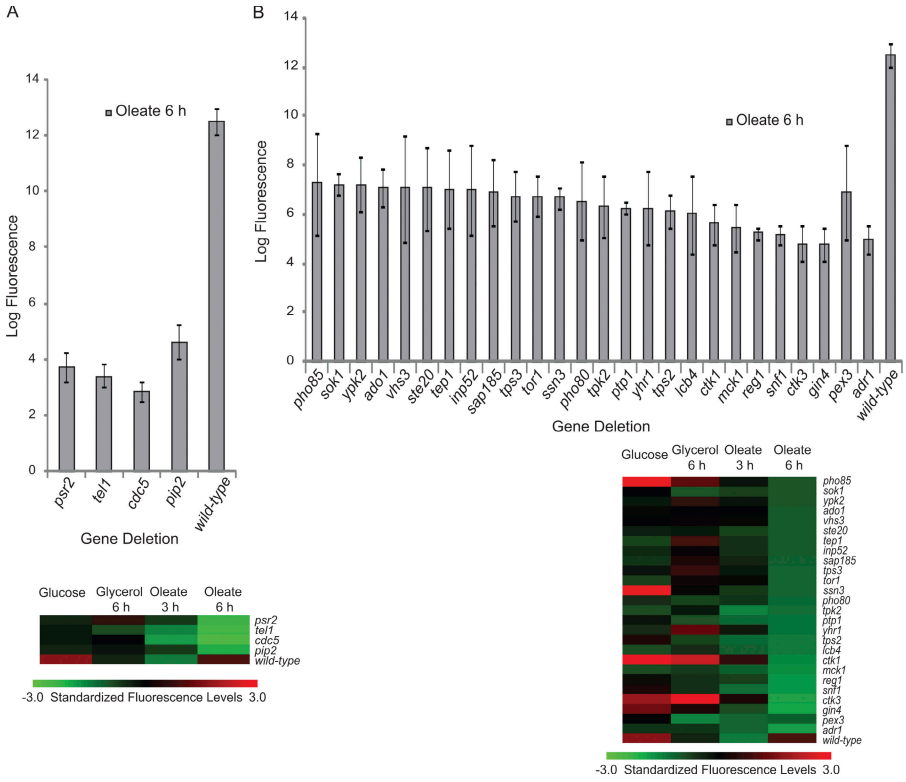

Figure 2. **Oleate-specific positive effectors.** (A) Pot1p-GFP levels in deletion mutants that result in a significant oleate-specific decrease in the levels of Pot1p-GFP (>2 SD). A strain deleted for *PIP2* is included as a control for negative effectors. The heat map shows that decreases in Pot1p-GFP levels are most pronounced after 6 h of oleate incubation. (B) Genes required for efficient oleate induction. Pot1p-GFP expression levels of deletion strains that showed decreases in Pot1p-GFP levels of between 1 and 2 SD below the population mean are shown. The heat map shows the relative intensities of Pot1p-GFP fluorescence among these strains under the four media conditions tested, with red and green indicating an increase and a decrease in fluorescence, respectively.

medium and then measuring levels of Pot1p-GFP by FACS analysis (Table S1, available at http://www.jcb.org/cgi/content/full/jcb.200710009/DC1), we were able to assign each signaling molecule as a positive, negative, or neutral effector of expression of Pot1p-GFP. By imaging analysis, we were also able to determine the effect that each gene deletion had on peroxisome biogenesis after induction of peroxisomes in oleate.

The *POT1* gene is normally repressed by glucose. Deletions that result in increased levels of Pot1p-GFP in glucose represent signaling proteins that function as positive effectors of glucose repression. This group includes *cax4Δ*, *ssn3Δ*, *elm1Δ*, *hrr25Δ*, *pho85Δ*, *dbf2Δ*, *ctk1Δ*, and *yck3Δ* (Fig. 1 A). Northern blot analysis in representative deletion strains demonstrates that the Pot1p-GFP reporter reflects mRNA levels expressed from *POT1* and another typical ORE-containing gene (Fig. S1 B, available at http://www.jcb.org/cgi/content/full/jcb.200710009/DC1).

This group of mutants defective in glucose repression can be further divided into three subgroups (Fig. 1 B). The first group (*elm1Δ*, *yck3Δ*, and *cax4Δ*) has increased expression in all conditions tested (glucose, glycerol, and oleate media). The second group (*ssn3Δ* and *ctk1Δ*) we term "uncoupled." These strains do not repress well in glucose and also respond poorly to oleate induction. The third group includes *hrr25Δ*, *pho85Δ*, and *dbf2Δ* strains. These cells respond poorly during the first 6 h of oleate-mediated induction but, unlike the uncoupled strains, Pot1p-GFP expression levels in these mutants increase moderately in response to oleate treatment and eventually reach wild-type levels (20 h; Fig. S2, available at http://www.jcb.org/cgi/content/full/jcb.200710009/DC1).

We next sought to identify genes responsible for the transition from the glucose-repressed state to either a glycerol-derepressed or an oleate-induced state. The panel of deletion strains was incubated in glucose-containing medium and then either in glycerol- or oleate-containing medium for 6 h (Fig. 1 C). Six genes (*SNF4*, *YPL236c*, *PIF1*, *SIT4*, *LCB5*, and *VPS34*) encoding signaling molecules were identified that, when deleted, caused dramatic defects in the ability of cells to transition from a glucose-repressed state regardless of whether this transition occurred in glycerol or oleate (>1 and 2 SD, respectively, below the population mean). That the same group of mutants was identified upon glycerol derepression or oleate induction suggests that the same process is illuminated in each case. We therefore attribute the phenotype of these mutants to their inability to effectively derepress the glucose state.

In contrast, deletions of three genes (*PSR2*, *TEL1*, and *CDC5*) were found to cause dramatic defects in oleate-induced expression but were not found to significantly (1 SD below the population mean) affect glycerol derepression. We consider these genes to be positive effectors of the oleate response (Fig. 2 A, heat map). These results show that, in addition to well studied glucose repression and derepression activities, there are specific signaling events required for oleate-mediated induction. We thus consider the core of the response to involve stepwise progression from glucose repression to glycerol depression to oleate induction, culminating in peroxisome biogenesis.

In addition to the three effectors with the most dramatic effects on oleate-mediated induction discussed in the previous paragraph, we also identified a larger group of oleate-specific positive effectors whose absence caused less pronounced reductions in Pot1p-GFP levels (between 1 and 2 SD below that of population mean; Fig. 2 B) but nonetheless were not identified as significant in the glycerol dataset (1 SD below the mean; Table S1).

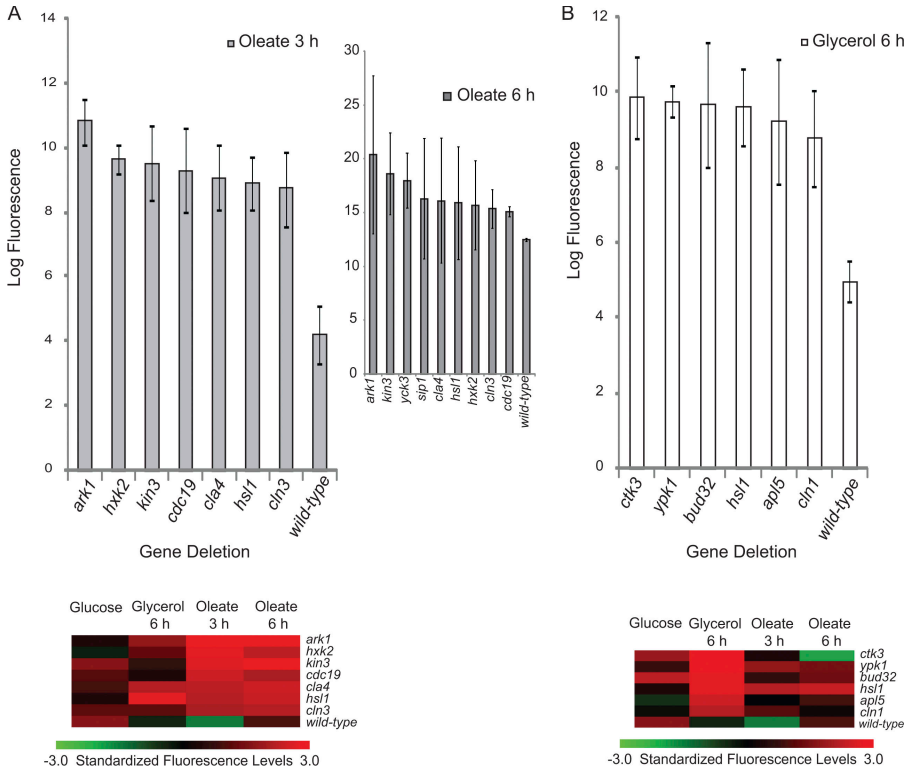

Figure 3. **Negative effectors.** (A) Oleate negative effectors. Pot1p-GFP levels in deletion mutants that exhibit an increase in Pot1p-GFP after 3 h of incubation in oleate are shown. At 6 h, the increase in Pot1p-GFP levels are generally higher than the population mean but show increased variability (right). (B) Glycerol negative effectors. The increase in Pot1p-GFP detected in deletion strains after 6 h of incubation in glycerol-containing medium is shown. Only the *hsl1Δ* mutant shows an up-regulation of Pot1p-GFP in both oleate and glycerol media, indicating that the normal role for *HSL1* is as a negative effector in both carbon sources. The heat map shows the relative intensities of Pot1p-GFP fluorescence in these strains under the four media conditions tested, with red and green indicating an increase and a decrease in fluorescence, respectively. Error bars show SD.

Interestingly, this group includes Snf1p. Snf1p has previously been shown to be required by cells to overcome glucose-mediated repression and to induce peroxisomes (Igual et al., 1992; Simon et al., 1992; Navarro and Igual, 1994) and the *POT1* gene in particular (Simon et al., 1992). Thus, although *snf1Δ* could be considered a "gold standard," *POT1* expression was not significantly different in *snf1Δ* cells compared with wild-type cells upon transition to glycerol, and the quantitative analysis reported here identified mutants that had more dramatic defects in Pot1p-GFP expression during derepression and oleate induction. Collectively, these data suggest that there is a core group of genes required for derepression and activation of oleate-induced genes but that the coordination of efficient cellular responses is contributed to differing extents by condition-specific effectors.

We also identified a group of negative regulators whose deletion caused an increase in the expression of Pot1p-GFP in oleate (Fig. 3 A). This group (*ark1Δ*, *hxk2Δ*, *kin3Δ*, *cdc19Δ*, *cla4Δ*, *hsl1Δ*, and *cln3Δ*) does not include those mutants that show increased levels of Pot1p-GFP in glucose (Fig. 1 A) but rather those deletion strains that show normal glucose-repressed levels of Pot1p-GFP before the transition to an oleate-induced state (Fig. 3 A). In line with their roles as negative regulators, the population variability of these deletion strains is high (Fig. 3 A, right). Likewise, a set of deletion strains exhibited increased Pot1p-GFP fluorescence (>1 SD above wild-type levels) upon transition to glycerol (Fig. 3 B). It is noteworthy that only *HSL1* negatively regulates both processes, again suggesting common stepwise elements to the derepression and activation of *POT1* in the context of coordination with other cellular processes.

Finally, we tested the panel of strains to search for those deletions that might allow cells to bypass the dominance of glucose repression. To do so, deletion strains were incubated in a medium combining 2% glucose and 1% oleate. Remarkably, none of the deletions tested showed a significantly increased level of Pot1p-GFP beyond that detected in the presence of glucose alone (unpublished data).

The phenotypes of the panel of deletion strains were also examined to define the role of individual members of the collection in peroxisome biogenesis. Peroxisome formation was observed by confocal fluorescence microscopy over a period of 20 h (Fig. S2). In wild-type cells, peroxisomes became visible as punctate structures by 2 h of incubation in oleate and proliferated extensively over time. To assess peroxisome formation, microscopic images were used to determine peroxisome volume and number, as well as peroxisome-specific fluorescence intensity, as distinct from overall cellular fluorescence intensity determined by FACS analysis (Fig. 4 A). Although the majority of mutants that were unable to produce normal peroxisomes were also identified by FACS analysis, morphological examination of the panel identified additional classes of signaling proteins required for normal peroxisome biogenesis. None of the mutants showed an observable mislocalization of the Pot1p-GFP reporter. Cluster analysis of the peroxisomal features associated with a panel of 225 deletion mutants revealed the presence of four dominant classes of mutant phenotypes (Fig. 4 B): Cluster I, with fewer and enlarged peroxisomes; Cluster II, with increased number but smaller volume of peroxisomes; Cluster III, with no detectable peroxisomes; and Cluster IV, with few small peroxisomes.

Membership in Clusters III and IV corresponds closely to mutants identified by FACS analysis. Cluster III represents those deletion strains that are unable to efficiently form peroxisomes and constitute positive effectors of peroxisome biogenesis.

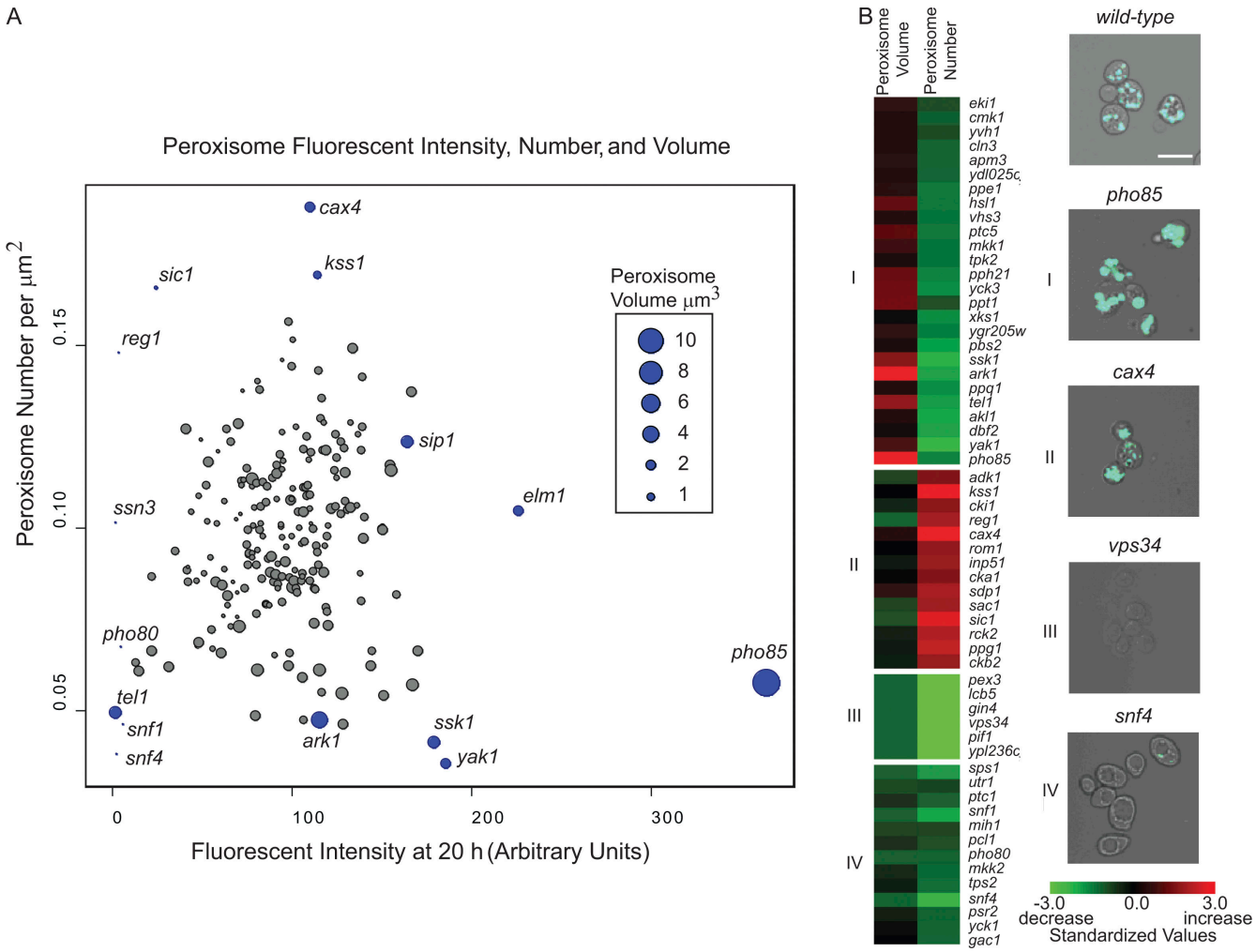

Figure 4. **Image analysis.** (A) Scatter plot of Pot1p-GFP fluorescence intensity of peroxisomes (arbitrary units) versus the number of peroxisomes per µm^2. The mean peroxisomal volume (µm^3) of each strain is also indicated. Blue circles are used to highlight those mutant strains referred to in the text, whereas gray circles are used to show the remaining population. (B) K-means clustering of standardized values for cell size, peroxisome volume, and number of peroxisomes per cell, with associated microscopic images of selected deletion strain cells at 20 h of oleate incubation. Bar, 10 µm. Clusters are discussed in the text. Cluster V is presented in Fig. S3 (available at http://www.jcb.org/cgi/content/full/jcb.200710009/DC1).

These correspond to strains identified by FACS analysis to have the largest decreases in Pot1p-GFP levels, with the exception of the *pex3Δ* strain, which cannot make peroxisomes and was included as a control. Cluster IV represents those strains that show peroxisome biogenesis phenotype defects resulting in a few small peroxisomes. These are deletions with FACS scores between 1 and 2 SD below wild-type levels but that over a 20-h time course are still able to form peroxisomal structures. Importantly, membership in this group also includes seven additional genes that were not identified as weak responders at the early time points investigated by FACS. We attribute the detection of these genes to the longer time periods used for microscopical analysis.

Clusters I and II reveal genes involved in biogenesis that could not be distinguished by FACS analysis alone. Cluster II represents those deletions that show increases in the numbers of peroxisomes present with modest effects on peroxisomal volume. The value and complementary nature of this analysis is illustrated by examining the Pot1p-GFP expression data for *reg1Δ* and *cax4Δ* cells. Although these mutants cluster adjacent to one another with respect to peroxisome morphology, they have distinctly different phenotypes with respect to Pot1p-GFP expression. Cells deleted for *REG1* are defective in producing Pot1p-GFP, whereas *cax4Δ* cells show increased production of Pot1p-GFP in glucose (Fig. 1 A).

Cluster I contains cells with fewer and enlarged peroxisomes. Of the 26 genes represented in Cluster I, 9 (35%) genes were found to also function in regulation of the Pot1p-GFP levels either positively or negatively (*ARK1*, *CLN3*, *DBF2*, *HSL1*, *PHO85*, *TEL1*, *TPS2*, *YCK3*, and *PHO80*). Deletions of *ARK1* and *PHO85* also regulate the size of the peroxisomes, with both deletions resulting in increases in peroxisomal volume with concomitant decreases in peroxisomal numbers. Peroxisomes in *pho85Δ* cells appear at early time points of oleate induction and, after extended incubation, result in large peroxisomal structures (20 h of oleate induction; Fig. 5 A). Similar, but less dramatic, results were observed in *sip1Δ* cells (Fig. S2). These data suggest that Pho85p and Sip1p act as repressors of peroxisome

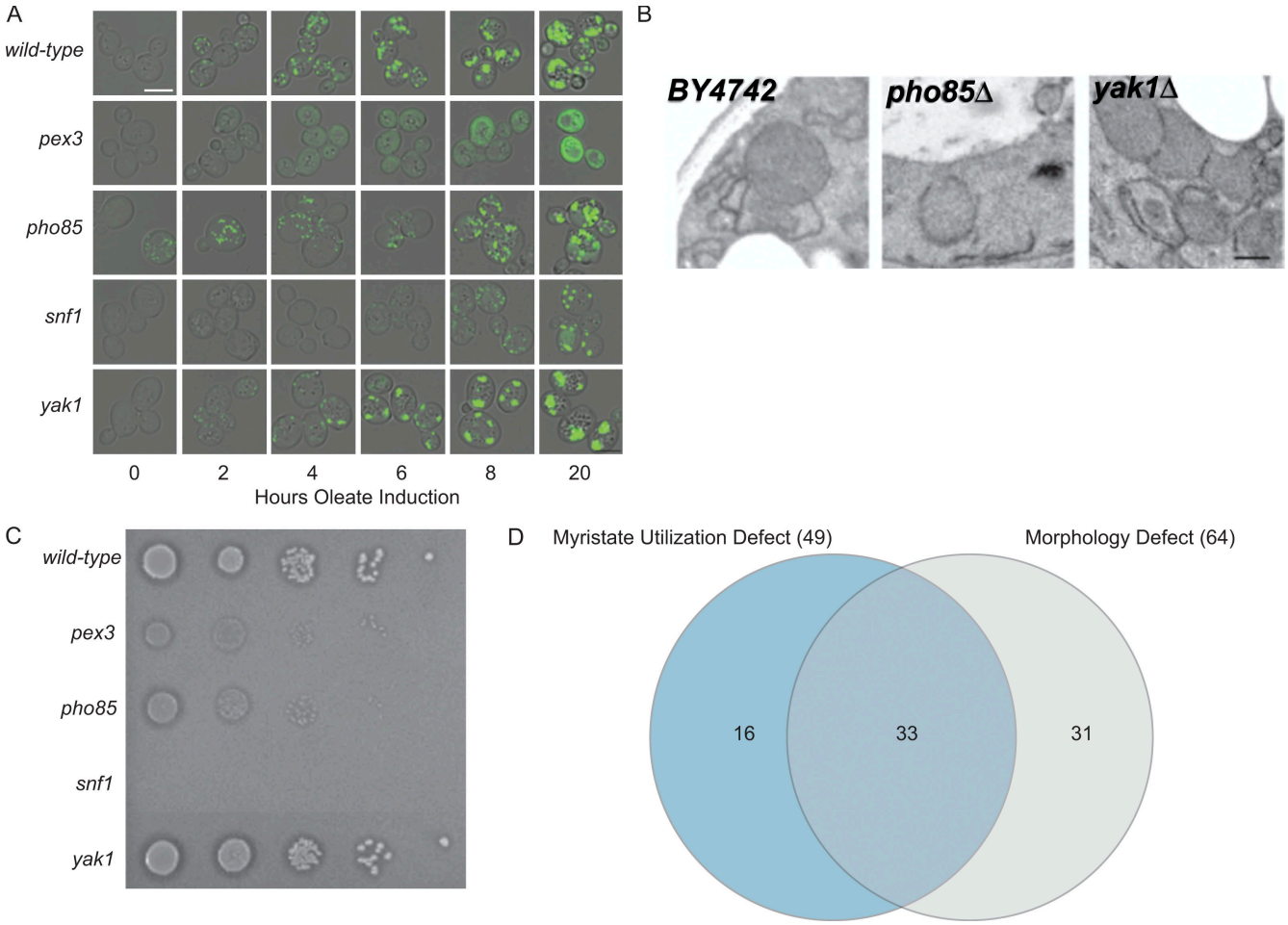

Figure 5. **Peroxisome biogenesis.** (A) Time course of peroxisome biogenesis over 20 h of incubation in oleate-containing YPBO medium. At 8 h, *yak1Δ* cells exhibit elongated peroxisomes, whereas *pho85Δ* cells present detectable peroxisomes before the oleate induction process (t = 0), and peroxisomes develop as smaller structures as compared with peroxisomes in wild-type cells. Bar, 10 μm. (B) Electron micrographs of peroxisomes in the wild-type strain *BY4742* and the *pho85Δ* and *yak1Δ* deletion strains. Cells deleted for *PHO85* show peroxisomes of reduced size, whereas *yak1Δ* cells show clustering of peroxisomes and thickened membranes between adherent peroxisomes. Bar, 0.25 μm. (C) Growth of strains on myristate-containing YPBM medium reveals reduced fatty acid metabolism in *pex3Δ*, *snf1Δ*, and *pho85Δ* strains. (D) Venn diagram showing the relationships between the number of deletion strains with myristate utilization defects, peroxisome morphology defects, and both defects.

biogenesis and that biogenesis and expression are coordinated by the activity of pathways involving these proteins.

The remaining 17 deletion strains of Cluster 1 also had fewer enlarged peroxisomes but were not detected to aberrantly affect *POT1* expression. This includes *yak1Δ* cells, which appeared to have few lobate peroxisomes after 8 h of oleate incubation. This interesting phenotype was confirmed and expanded upon by ultrastructural analyses (Fig. 5 B). In contrast to the wild-type strain and another Cluster 1 strain, *pho85Δ*, peroxisomes of *yak1Δ* cells were observed to cluster and to sometimes share a common membrane (Fig. 5 B).

Peroxisome functionality was assessed by growth of cells on solid medium (YPBM) containing the fatty acid myristate as the principal carbon source (Smith et al., 2006). Cells with a functional peroxisomal β-oxidation system grow on YPBM, and their consumption of myristate can be assessed by the formation of haloes around colonies (Fig. 5 C; and Table S2, available at http://www.jcb.org/cgi/content/full/jcb.200710009/DC1). 49 mutants were unable to efficiently metabolize myristic acid, and two thirds of these strains also showed morphological defects (Fig. 5 D). Of the 64 strains with morphological defects, approximately half had fatty acid metabolism defects. Thus, it is difficult to predict functionality based on morphology alone. Indeed, although *pho85Δ* and *yak1Δ* cells have similar peroxisomal morphology defects, they have distinctly different myristic acid metabolism properties. This is similar to the situation with classically defined *pex* mutants. Although the first *pex* mutants were identified by their inability to grow on fatty acids, many of the *pex* mutants identified more recently are able to metabolize fatty acids and, thus, do not have major peroxisomal assembly or protein import defects.

Discussion

We have systematically and quantitatively surveyed the functional consequences of deletions of the majority of the known yeast kinases, phosphatases, and cyclins encoded by the *S. cerevisiae* genome with respect to their roles as positive, negative, or neutral

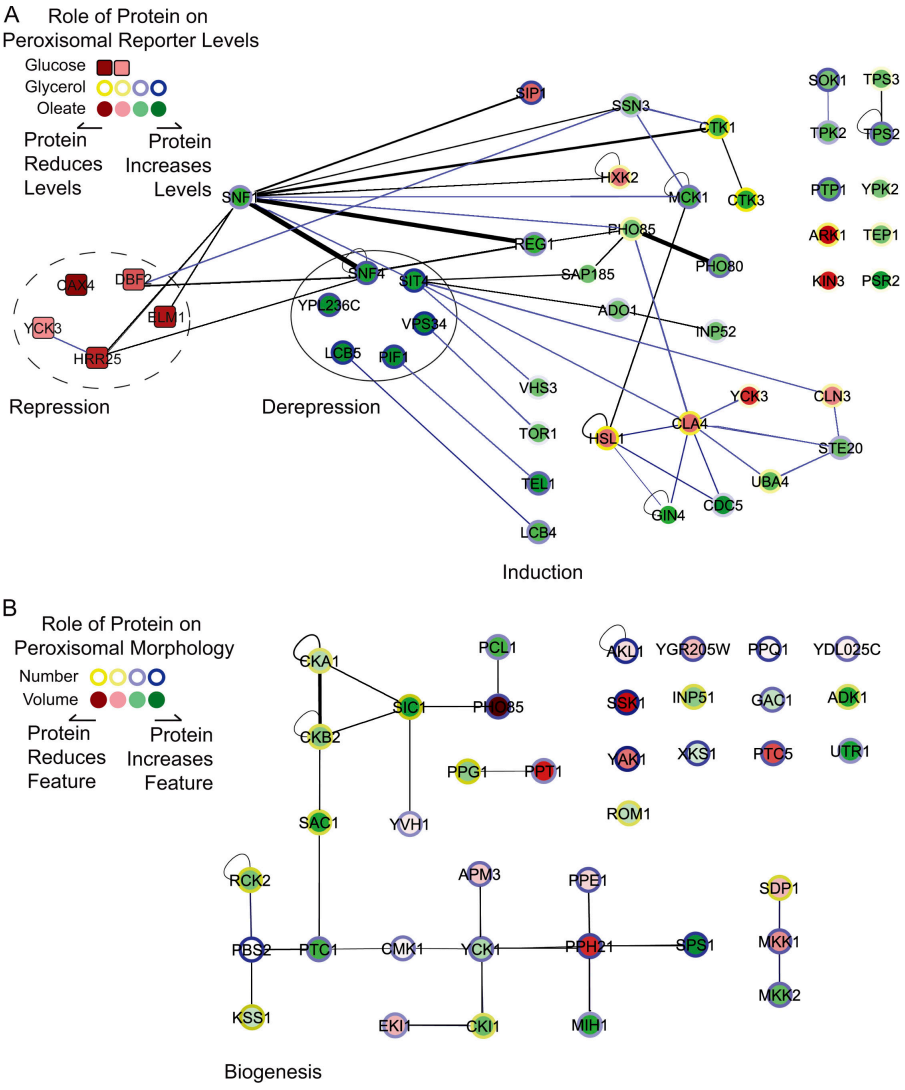

Figure 6. **Core signaling molecules of Pot1p expression and peroxisome biogenesis.** (A) Representation of the genes discussed in the text showing the oleate activation network. Included are genes involved in glucose repression, together with the overlap between the glycerol derepression and oleate activation datasets. Genes are represented by shapes, whereas interactions between gene products are represented by lines. For both A and B, lines are shown as black for physical interactions and blue for genetic interactions. Increasing thickness of lines reflects increasing published interactions. Genes required for repression in glucose are shown by squares, whereas reporter levels in the deletion strain of a given gene in glycerol are indicated by the oval borders. Reporter levels of the deletion strains after incubation in oleate are represented by circles. A color gradient between green and red is used to represent the strength effect of the gene products on expression of Pot1p-GFP for both oleate activation and glucose repression. Red is used for those gene products that function to reduce the levels of Pot1p-GFP, whereas green is used for those gene products whose normal function is to increase the levels of Pot1p-GFP. A color gradient between blue and yellow is used to represent the strength of the effect of these gene products on Pot1p-GFP after 6 h of glycerol incubation. Blue is used to indicate those gene products that function as positive effectors of Pot1p-GFP expression, whereas yellow is used to indicate those gene products that function as negative effectors of Pot1p-GFP expression. (B) Representation of the genes that form the peroxisome biogenesis network. Genes are represented by circles and interactions between gene products are represented by lines. Peroxisome volume is indicated by circles, whereas peroxisome number is indicated by the circle border. A color gradient between green and red circles represents the strength of regulation of peroxisome volume, whereas a color gradient between blue and yellow circle borders represents the strength of regulation of peroxisome number. Those gene products which are negative effectors of peroxisome volume are shown in red, whereas those that are positive effectors are shown in green. Those gene products which are negative effectors of peroxisome number are represented by yellow circle borders, whereas those that are positive effectors are represented by blue circle borders. *PHO85* is included in this network because of its role in biogenesis.

effectors of oleate-mediated peroxisome biogenesis during oleate activation. To evaluate the specific role of each signaling protein, the process has been dissected into four fundamental steps: repression of genes for peroxisome-related proteins by glucose, derepression by transfer of cells to glycerol, oleate-mediated activation of gene expression, and production of the organelle itself. Our findings indicate that although the majority of signaling proteins tested do not significantly affect the process, specific and common key signaling proteins regulate each of the four steps. To place these data in the context of our current understanding of the roles of each protein, networks of significant signaling molecules in these processes were overlaid with the physical and genetic interactions between each signaling component (Fig. 6) together with the Gene Ontology (GO) annotations (https://www.proteome.com/proteome/YPD) for these proteins, which were used as an aid for understanding their reported roles. Oleate-induced peroxisomal biogenesis is preceded by signaling mechanisms to transition cells in a stepwise fashion from a glucose-repressed to an oleate-activated state. This study identifies signaling machineries that specify the requirements of the early and late biogenesis events of peroxisomes and groups of global regulators of glucose repression, cell cycle pathways that differentially activate genes encoding peroxisomal proteins, and mediators controlling the phosphorylation status of lipids. These results are summarized in Fig. 6, which presents systems level schematics of signaling protein networks controlling oleate-mediated induction of Pot1p-GFP and peroxisome biogenesis (Table I).

Repression

Glucose-mediated repression of the Pot1p-GFP peroxisomal reporter requires eight of the signaling molecules tested (Fig. 6 A). Five were specifically required for repression (Fig. 6 A, circled), and three (Ctk1p, Pho85p, and Ssn3p) were also implicated in oleate activation. Snf1p is a well characterized protein required to overcome glucose repression (Igual et al., 1992; Navarro and Igual, 1994). Accordingly, the positive effectors

Table I. **Gene deletions producing a phenotype in a given process (repression, depression, induction, or biogenesis) grouped according to their roles at a systems level**

	Glucose repression	Glycerol derepression	Oleate induction	Peroxisome biogenesis
Positive process effectors	cax4	lcb5	pho85	akl1
	ssn3	pif1	sdk1	apm3
	elm1	sit4	ypk2	cmk1
	hrr25	snf4	ado1	eki1
	pho85	vps34	vhs3	gac1
	dbf2	ypl236c	ste20	mih1
	ctk1		tep1	mkk1
	yck3		inp52	mkk2
			sap185	pbs2
			tps3	pcl1
			tor1	ppe1
			ssn3	pph21
			pho80	ppq1
			tpk2	ppt1
			ptp1	ptc1
			yhr1	ptc5
			tps2	sps1
			lcb4	ssk1
			ctk1	utr1
			mck1	xks1
			reg1	yak1
			snf1	yck1
			ctk3	ydl025c
			gin4	ygr205w
			psr2	yvh1
			tel1	
			cdc5	
Negative process effectors		ctk3	ark1	adk1
		ypk1	hxk2	cka1
		bud32	kin3	ckb2
		hsl1	cdc19	cki1
		apl5	cla4	inp51
		cln1	hsl1	kss1
			cln3	ppg1
				rck2
				rom1
				sac1
				sdp1
				sic1

of repression consist of several Snf1p-interacting proteins, including Ssn3p, Ctk1p, Elm1p, Pho85p, and Hrr25p (Fig. 6 A), as well as two proteins, Dbf2p and Yck3p, which are separated with respect to their interaction with Snf1p by intermediary proteins. The role of Cax4p in glucose repression is less clear, as it has not been previously implicated in this process and is functionally annotated as being involved in sphingolipid metabolism.

Deletions of most genes in this class of positive effectors of glucose repression are unaffected by oleate induction. This is not surprising, because the glucose-repressed and oleate-induced states are separable. However, unlike other members of the group, strains deficient in Pho85p, Ssn3p, and Ctk1p are defective in both glucose repression and oleate-mediated induction. Pho85p plays complex roles in repression and induction of the *POT1* locus, as well as a role in biogenesis of peroxisomes themselves (see Biogenesis). Ssn3p and Ctk1p are components of the RNA polymerase II complex and, in agreement with the data presented here, have previously been shown to both positively and negatively influence gene expression (Liao et al., 1995; Hengartner et al., 1998).

Derepression

Most genes encoding peroxisomal proteins are repressed in glucose and activated in oleic acid (Smith et al., 2002). We consider the transition between these states to involve two steps, i.e., depression followed by activation. To identify proteins involved in each of these steps, cells were incubated in glucose and then glycerol to identify genes involved in derepression and in glucose and then oleic acid to identify genes involved in both derepression and activation. Proteins involved in both processes

are therefore considered responsible for transition to the derepressed state, whereas proteins involved in only oleate induction are considered specific to induction.

Glycerol-mediated derepression, unlike glucose repression, is mediated by signaling proteins whose GO annotations are distributed between numerous processes, for example, vacuolar protein sorting, cell cycle, phosphatidylinositol signaling, and sphingolipid biosynthesis. The lack of specificity in the annotations may speak to the numerous processes that are preceded by relief of glucose repression, complexity of the transition to the derepressed state, the lack of publicly available information with regards to this process, or all three points. As discussed in the previous section, Snf1p is well characterized as being required for expression of glucose-repressed genes upon derepression, including the *POT1* gene (Einerhand et al., 1991; Igual et al., 1992; Simon et al., 1992). Although we detect considerable defects in this transition for *snf1Δ* mutants, this analysis identified six proteins whose absence results in defects more severe than those observed for *snf1Δ* cells. Snf4p is the γ-subunit of the active Snf1p kinase complex (Simon et al., 1992; Elbing et al., 2006). Vps34p is involved in glucose repression of the *ADH2* gene encoding alcohol dehydrogenase (Voronkova et al., 2006), whereas Sit4p, Lcb5p, Pif1p, and Ypl236p have not previously been implicated in the expression of glucose-repressed genes.

The derepression component of the oleate activation network (Fig. 6 A) reveals previously uncharacterized roles for signaling molecules, including the sphingolipid metabolism kinase Lcb5p and a phosphatidylinositol kinase involved in vacuolar transport, Vps34p. Sphingolipids are a class of lipids that are known to play roles in signal transmission and are important regulators of the cell cycle (for reviews, see Hannun and Obeid, 2002; Fernandis and Wenk, 2007). Phosphatidylinositols are, like sphingolipids, becoming recognized as more than structural components of lipid bilayers. They can be metabolized quickly and the products act as second messengers (for review, see Strahl and Thorner, 2007). Our data show that Lcb5p and Vps34p are critical effectors for the transition of the *POT1* locus to a derepressed or induced state. Furthermore, these data show that genes annotated in processes as diverse as sphingolipid metabolism, phosphatidylinositol metabolism, and vacuolar protein sorting play significant roles in derepression.

YPL236c is a previously uncharacterized gene whose deletion has a profound effect on Pot1p-GFP expression during derepression. High-throughput screens have localized the protein to mitochondria and the vacuole (Kumar et al., 2002; Huh et al., 2003). Ypl236p might interact with Ufd2p, an E4 ligase involved in multiubiquitination and can be phosphorylated and palmitoylated (Zhu et al., 2000; Roth et al., 2006). No function has been attributed to Ypl236p, but based on the data presented here, we propose that Ypl236p is an important positive effector of transcription of glucose-repressed genes upon derepression or induction.

Induction

We and others have begun to characterize the transcriptional regulatory network of oleate induction in *S. cerevisiae* (Smith et al., 2002, 2007; for review see Gurvitz and Rottensteiner, 2006). These studies have focused on the function of four transcription factors, Oaf1p, Pip2p, Adr1p, and Oaf3p, governing the response. In this network, Adr1p induces expression of *PIP2*. Pip2p forms a heterodimer with constitutively present Oaf1p, which is activated by binding fatty acids directly (Phelps et al., 2006). Oaf3p appears to modulate the response (Smith et al., 2007). The signaling response to oleate is less well characterized. It is apparent from the data shown here that in addition to Oaf1p binding oleate, a host of signaling proteins is required for efficient induction of fatty acid–responsive genes and peroxisome formation itself. For example, Psr2p is a plasma membrane phosphatase that, along with Whi2p, is thought to modulate the general stress response by regulating the activity of Msn2p (Kaida et al., 2002). The activity of Psr2p does not appear to be important for depression but is required for oleate-mediated induction. The general stress response is tightly integrated with the oleate response (Koerkamp et al., 2002; Smith et al., 2002), and our data suggest that Psr2p is an important molecular link between these two processes.

Several other highly connected proteins are also required for oleate induction, but not glycerol derepression, of the Pot1p-GFP reporter (Fig. 6 A). As expected, this group includes components that interact with Snf1p, but it also includes a surprising number of proteins involved in regulation of the cell cycle (Cdc5p, Cln3p, Gin4p, Hsl1p, Kin3p, Mck1p, Pho80p, Pho85p, Sap185p, Ste20p, and Vhs3p). This may reflect a dramatic shift in the metabolic state of cells in glycerol as compared with oleate, as well as the coordination required for an extended cell cycle (∼1.5–2 h in glucose vs. >6 h in oleate; Koerkamp et al., 2002; Smith et al., 2002). The other major annotation in this network is that of phosphatidylinositol metabolism, which contains four genes required for oleate induction. These proteins function as phosphatidylinositol kinases in a variety of processes, including actin polymerization (Inp52p), telomere maintenance (Tel1p), transcriptional control (Tor1p), and actin polarity and membrane targeting (Cla4p). The precise role of these proteins in the context of oleate induction is unclear; however, it is clear that they function to enhance oleate responsiveness. From our data, we conclude that coordinated activation of the glucose regulation, cell cycle regulation, and phosphatidylinositol metabolism networks is necessary for efficient expression of oleate-induced peroxisomal proteins.

Biogenesis

Microscopy was used to identify those signaling proteins required for the formation of morphologically normal peroxisomes. Because peroxisome formation lies downstream of gene transcription, in our analysis, we subtracted the signaling proteins involved in the transcriptional response from the entire repertoire of signaling proteins to identify those proteins that specifically effect peroxisome formation (Fig. 6 B and Table I). We refer to this group as biogenesis-specific effectors. Three primary subgroups (i.e., those involved in actin regulation or phosphatidylinositol metabolism and "other," those proteins with disparate GO annotations of effectors) were revealed by this analysis. There are six actin regulating molecules (Inp51p, Mkk1p, Mkk2p, Pph21p, Rom1p, and Sac1p), and much of the function of these signaling proteins is mediated through the action of Rho regulators. Rho1p has been shown to localize to, and be required for, the normal biogenesis of peroxisomes

through its regulation of the polymerization state of actin on the peroxisome (Marelli et al., 2004). With respect to the second major subgroup involved in phosphatidylinositol metabolism (Ckl1p, Cmk1p, Inp51p, Kss1p, Sac1p, Sps1p, and Vps34p), it is interesting to note that certain phosphoinositides have been shown to be required for peroxisomal precursor fusion (Boukh-Viner et al., 2005). This fact, and the diminutive size of peroxisomes in strains such as *kss1Δ*, *sac1Δ*, and *vps34Δ*, whose encoded proteins have lipid kinase and phosphatase activities (in addition to the actin regulatory activity of both Sac1p and Inp51p), suggest that these peroxisomal forms may be trapped in an immature stage in early biogenesis. As peroxisomal fusion is a poorly characterized process, the mutant phenotypes detected here provide candidate molecules for investigation toward a mechanistic understanding of the process. The large number of biogenesis effector proteins with disparate GO annotations likely reflects the complexity of biogenesis and the host of processes required for development of the organelle.

The phenotypes identified by confocal microscopy are similar to those observed in peroxisome division mutants, i.e., a few large peroxisomes or many small peroxisomes (Fig. 4 B, Clusters I and II) or are mutants with no or little detectable induction of peroxisomes (Fig. 4 B, Clusters III and IV), which possibly represents mutants with very low levels of Pot1p-GFP. These data suggest that, in particular for proteins in clusters I and II, biogenesis that is regulated by this group of signaling proteins involves growth and division rather than de novo biogenesis of peroxisomes from the ER (Hoepfner et al., 2005; Tam et al., 2005). However, defects at the early stages of biogenesis, for example, fission from the ER, cannot be ruled out at this point, and feedback between the ER and proteins involved in peroxisome biogenesis remains an uninvestigated possibility.

None of the signaling mutants tested led to cytosolic accumulation of Pot1p-GFP, suggesting that peroxisomal matrix protein import, per se, is not altered. However, there are at least two pathways for matrix protein import. PTS2-containing proteins like Pot1p are imported by Pex7p, whereas PTS1-containing proteins are imported by Pex5p and membrane proteins are integrated into the organelle by yet additional mechanisms (for reviews see Rayapuram and Subramani, 2006; Platta and Erdmann, 2007). Therefore, it is possible that some of the mutants examined have PTS1, membrane protein, or cargo-specific peroxisomal protein targeting, transport, or membrane protein integration defects.

The size and abundance of peroxisomes can be regulated by the levels of the matrix proteins they contain (Chang et al., 1999; Smith et al., 2000, van Roermund et al., 2000). In our data, we see evidence of this phenomenon. For example, the increased levels of Pot1p-GFP seen in the *cax4Δ* strain result in a dramatic increase in the number of peroxisomes, whereas cells deleted for *SNF1* or *SNF4*, among other genes, show decreased levels of Pot1p-GFP together with concomitant decreases in peroxisome volume and number (Fig. 5 B and Fig. S2). As mentioned previously, because these mutants are affected in their Pot1p-GFP levels, they were not included as biogenic effectors, a group that we restrict to mutants that specifically exhibit altered peroxisome morphology.

An exception to this rule is Pho85p, which plays a complex role in repression, induction, and biogenesis. In glucose conditions, levels of Pot1p-GFP are high in *pho85Δ* cells, which is in good agreement with confocal data (Table S2), demonstrating a role for Pho85p as a positive effector of glucose-mediated repression. By 6 h of oleate incubation, the levels of Pot1p-GFP in *pho85Δ* cells are still 1 SD below those observed in wild-type cells, yet visual analysis revealed the formation of multiple small peroxisomes (Fig. S2 and Table S2), implying that peroxisome biogenesis is premature in the *pho85Δ* strain and that Pho85p acts as a negative effector of peroxisome biogenesis. After extended periods of oleate induction, Pot1p-GFP levels in *pho85Δ* cells approach those of wild-type cells, and by 20 h in YPBO, the multiple small peroxisomes found in *pho85Δ* cells cluster and present as large peroxisomes by fluorescence microscopy (Fig. 4 A) and as multiple adjacent small peroxisomes by EM (Fig. 5 C). Thus, Pho85p appears to act as a positive effector of glucose-mediated repression of Pot1p-GFP expression (hence the up-regulation of Pot1p-GFP in *pho85Δ* cells in glucose medium), a positive effector of efficient Pot1p-GFP expression during oleate induction (hence the diminished levels of Pot1p-GFP in *pho85Δ* cells after 6 h in oleate medium), and a negative effector of biogenesis (hence the premature appearance of peroxisomes in *pho85Δ* cells in oleate medium). These data show that Pho85p is a unique protein in the overall process, and its various functions remain fertile ground for further investigation.

An interesting feature revealed by our data is the possibility of a feedback mechanism between peroxisomes and the nucleus. In *pex3Δ* cells in which no peroxisomal structures can be observed, there is a significant decrease in the levels of Pot1p-GFP after 6 h of oleate induction (Fig. 2 B). This observation raises the intriguing possibility that efficient transcription, at least initially, may be regulated by the peroxisome itself; however, further study is required.

Despite recent advances in the analysis of the kinomes of various organisms (Pelkmans et al., 2005; Ptacek et al., 2005), this study is, to our knowledge, the first global investigation of both kinase and phosphatase activities in a complex biological phenomenon, the biogenesis of an organelle. This work is also the first study of the signaling mechanisms underlying the development of an organelle from gene transcription through to the formation of intact mature and functioning structures. By using a systematic and quantitative approach, we have delineated the signaling proteins required for glucose-mediated transcriptional repression, transition from a repressed to a derepressed state in glycerol and oleate, induction in response to oleate exposure, and biogenesis of peroxisomes with respect to the size, number, and timing of the development of the organelle. The dynamics of peroxisomes in wild-type cells and the complexity of phenotypes uncovered in our strain collection are suggestive of a stringent integration of signaling events in the temporal and spatial control of peroxisome assembly. Collectively, our data demonstrate both the complexity and convergence of signaling pathways in organelle biogenesis. This work thus provides a framework from which the stepwise function of these pathways and processes can be investigated and determined.

Materials and methods

Yeast cell culture and genetic manipulation

All *S. cerevisiae* strains used in this study are listed in Table S3 (available at http://www.jcb.org/cgi/content/full/jcb.200710009/DC1). Strains were cultured at 30°C in the following media: YPD (1% yeast extract, 2% peptone, and 2% glucose), YPBO (0.3% yeast extract, 0.5% peptone, 0.5% potassium phosphate buffer, pH 6.0, 0.5% Tween 40, and 1% oleic acid), YPBM (0.67% yeast nitrogen base, 0.1% yeast extract, 0.5% potassium phosphate buffer, pH 6.0, 0.5% Tween 40, and 0.125% myristic acid), YPBD (0.67% yeast nitrogen base, 0.1% yeast extract, 0.5% potassium phosphate buffer, pH 6.0, 0.5% Tween 40, and 2% glucose), and SSM (Complete supplement medium [BIO101], 0.09% KH_2PO_4, 0.023% K_2HPO_4, 0.05% $MgSO_4$, and 0.35% $(NH_4)_2SO_4$). To construct strains expressing the Pot1p-GFP chimera, the *POT1* gene was tagged at its 3′ end through homologous recombination with a PCR-based strategy in frame with the sequence encoding *Aequorea victoria* GFP (Scholz et al., 2000). All genomic integrations were confirmed by PCR. Integrations were also verified by sequencing. Allelism for strains with significant phenotypes, as measured here, was established by complementation analysis.

FACS

Cells of deletion strains were grown in YPBD to mid-log phase in 96-well deep-well plates, pelleted, washed with water, resuspended in the same volume of YPBO or YPBG, and incubated with shaking for 3 or 6 h as indicated at 30°C. Cells were then processed by removal of the medium, fixation in 3.7% formaldehyde for 30 min, and resuspension in water and analyzed with a FACSCalibur (BD Biosciences) with the following parameters: forward scatter, E0 haploid linear scale; side scatter, 520 V linear scale; fluorescence, 490 V logarithmic scale. Cells were loaded onto the FACSCalibur using the high throughput sampler (BD Biosciences). The high throughput sampler was run in standard mode using a 96-well flat-bottomed plate and was set to sample 10 µl at a rate of 2 µl/s. All experiments were replicated a minimum of three times with a minimum of two technical replicates per biological replicate.

Confocal fluorescence microscopy

To visualize the Pot1p-GFP chimera in time-course experiments, strains were grown to midexponential phase in YPBD, resuspended in the same volume of YPBO, and incubated for 2, 4, 6, 8, and 20 h in YPBO at 30°C. Five images per time point per strain were captured randomly with a Plan-Apochromat 63×/1.4 NA oil differential interference contrast objective on an inverted microscope (Axiovert 200; Carl Zeiss, Inc.) equipped with a confocal scanner (LSM 510 META; Carl Zeiss, Inc.). GFP was excited with a 488-nm laser and its emission was collected using a 505-nm long-pass filter. Images were captured at 23°C with the microscope pinhole adjusted to 1 Airy unit. Total peroxisome induction and peroxisome volumes were determined with Metamorph Imaging System 6.3 software (MDS Analytical Technologies). The channels of the LSM images were split, the transmission channel was processed with "Flatten Background" and "Median" filters and binarized, and the total and mean cell areas in the image plane were recorded for each strain. Peroxisome induction was calculated as pixel intensity of the green channel per cell. Peroxisome volumes were recorded in the green channel using Metamorph's "threshold image" and "count cells" functions. Peroxisome numbers per cell at 20 h of induction were manually counted in at least 100 cells per strain using the spot counting tool of the Imaris 5.0 imaging software (Bitplane). All other computational analyses were performed with Origin 7.0 software (OriginLab).

EM

Fixation and processing of cells for EM were performed as described previously (Eitzen et al., 1997).

Clustering

Pot1p-GFP fluorescence. Data were converted by standardizing the raw log fluorescence for each experiment according to the equation $Z = (X - \mu)/\sigma$, where X = mean log fluorescence of a given deletion, μ = the population mean fluorescence, and σ = the population mean SD. Heat maps were generated using the mean standardized values in the TMEV program (Saeed et al., 2003, 2006) and standardized using a range of −3 and 3 for all FACS data.

Imaging data. Imaging data were comprised of cell area, peroxisome volume, and number of peroxisomes for each deletion strain after 20 h of induction in YPBO. Values were standardized using the equation in the previous section and clustered with the TMEV program using k-means clustering, choosing 10 clusters as the initial parameter. Similar clusters were merged, leaving a total of five clusters.

Cytoscape analysis

Interaction data were obtained through the *Saccharomyces* Genome Database (http://www.yeastgenome.org). Interaction data for each group (Table I) were acquired using the *Saccharomyces* Genome Database batch download tool on December 8, 2007. High-throughput physical interactions were removed from the interaction dataset. Interactions were visualized using Cytoscape 2.5.1 (Shannon et al., 2003).

Online supplemental material

Fig. S1 shows that the regulation of peroxisomal loci is conserved. Fig. S2 shows confocal images of oleate induction of the Pot1p-GFP chimera in the deletion strains over a 20-h time course. Fig. S3 shows the k-means clustering of peroxisome number and volume determined by analysis of confocal images. Table S1 contains the data for the FACS analysis of the deletion strains. Table S2 contains the data for the imaging-based quantification of peroxisome biogenesis. Table S3 lists the *S. cerevisiae* strains used in this study. Online supplemental material is available at http://www.jcb.org/cgi/content/full/jcb.200710009/DC1.

We thank Drs. Andrew Simmonds and Xuejun Sun for help with image analysis. The technical assistance of Honey Chan, Hanna Kroliczak, Richard Poirier, Elena Savidov, Dwayne Weber, and Mark Fuller and the computational assistance of Dorian Rachubinski are greatly appreciated.

This work was supported by grant 53326 from the Canadian Institutes of Health Research to R.A. Rachubinski and by grants RO1 GM067228, RR022220, and PM50 GMO76547 from the National Institutes of Health to J.D. Aitchison. R.A. Saleem is a recipient of a Canadian Institutes for Health Research Postdoctoral Fellowship. C.M. Dobson is the recipient of a Full-Time Fellowship from the Alberta Heritage Fund for Medical Research. R.A. Rachubinski is Canada Research Chair in Cell Biology and an International Research Scholar of the Howard Hughes Medical Institute.

Submitted: 1 October 2007
Accepted: 24 March 2008

References

Baumgartner, U., B. Hamilton, M. Piskacek, H. Ruis, and H. Rottensteiner. 1999. Functional analysis of the Zn_2Cys_6 transcription factors Oaf1p and Pip2p. Different roles in fatty acid induction of β-oxidation in *Saccharomyces cerevisiae*. *J. Biol. Chem.* 274:22208–22216.

Boukh-Viner, T., T. Guo, A. Alexandrian, A. Cerracchio, C. Gregg, S. Haile, R. Kyskan, S. Milijevic, D. Oren, J. Solomon, et al. 2005. Dynamic ergosterol- and ceramide-rich domains in the peroxisomal membrane serve as an organizing platform for peroxisome fusion. *J. Cell Biol.* 168:761–773.

Chang, C.C., S. South, D. Warren, J. Jones, A.B. Moser, H.W. Moser, and S.J. Gould. 1999. Metabolic control of peroxisome abundance. *J. Cell Sci.* 112:1579–1590.

Einerhand, A.W., T.M. Voorn-Brouwer, R. Erdmann, W.H. Kunau, and H.F. Tabak. 1991. Regulation of transcription of the gene coding for peroxisomal 3-oxoacyl-CoA thiolase of *Saccharomyces cerevisiae*. *Eur. J. Biochem.* 200:113–122.

Eitzen, G.A., R.K. Szilard, and R.A. Rachubinski. 1997. Enlarged peroxisomes are present in oleic acid-grown *Yarrowia lipolytica* overexpressing the *PEX16* gene encoding an intraperoxisomal peripheral membrane peroxin. *J. Cell Biol.* 137:1265–1278.

Elbing, K., E.M. Rubenstein, R.R. McCartney, and M.C. Schmidt. 2006. Subunits of the Snf1 kinase heterotrimer show interdependence for association and activity. *J. Biol. Chem.* 281:26170–26180.

Erdmann, R., and W. Schliebs. 2005. Peroxisomal matrix protein import: the transient pore model. *Nat. Rev. Mol. Cell Biol.* 6:738–742.

Fernandis, A.Z., and M.R. Wenk. 2007. Membrane lipids as signaling molecules. *Curr. Opin. Lipidol.* 18:121–128.

Gurvitz, A., and H. Rottensteiner. 2006. The biochemistry of oleate induction: transcriptional upregulation and peroxisome proliferation. *Biochim. Biophys. Acta.* 1763:1392–1402.

Hannun, Y.A., and L.M. Obeid. 2002. The ceramide-centric universe of lipid-mediated cell regulation: stress encounters of the lipid kind. *J. Biol. Chem.* 277:25847–25850.

Hengartner, C.J., V.E. Myer, S.M. Liao, C.J. Wilson, S.S. Koh, and R.A. Young. 1998. Temporal regulation of RNA polymerase II by Srb10 and Kin28 cyclin-dependent kinases. *Mol. Cell.* 2:43–53.

Hiltunen, J.K., A.M. Mursula, H. Rottensteiner, R.K. Wierenga, A.J. Kastaniotis, and A. Gurvitz. 2003. The biochemistry of peroxisomal β-oxidation in the yeast *Saccharomyces cerevisiae. FEMS Microbiol. Rev.* 27:35–64.

Hoepfner, D., D. Schildknegt, I. Braakman, P. Philippsen, and H.F. Tabak. 2005. Contribution of the endoplasmic reticulum to peroxisome formation. *Cell.* 122:85–95.

Huh, W.K., J.V. Falvo, L.C. Gerke, A.S. Carroll, R.W. Howson, J.S. Weissman, and E.K. O'Shea. 2003. Global analysis of protein localization in budding yeast. *Nature.* 425:686–691.

Igual, J.C., C. Gonzalez-Bosch, L. Franco, and J.E. Perez-Ortin. 1992. The *POT1* gene for yeast peroxisomal thiolase is subject to three different mechanisms of regulation. *Mol. Microbiol.* 6:1867–1875.

Kaida, D., H. Yashiroda, A. Toh-e, and Y. Kikuchi. 2002. Yeast Whi2 and Psr1-phosphatase form a complex and regulate STRE-mediated gene expression. *Genes Cells.* 7:543–552.

Karpichev, I.V., and G.M. Small. 1998. Global regulatory functions of Oaf1p and Pip2p (Oaf2p), transcription factors that regulate genes encoding peroxisomal proteins in *Saccharomyces cerevisiae. Mol. Cell. Biol.* 18:6560–6570.

Koerkamp, M.G., M. Rep, H.J. Bussemaker, G.P. Hardy, A. Mul, K. Piekarska, C.A. Szigyarto, J.M. De Mattos, and H.F. Tabak. 2002. Dissection of transient oxidative stress response in *Saccharomyces cerevisiae* by using DNA microarrays. *Mol. Biol. Cell.* 13:2783–2794.

Kumar, A., S. Agarwal, J.A. Heyman, S. Matson, M. Heidtman, S. Piccirillo, L. Umansky, A. Drawid, R. Jansen, Y. Liu, et al. 2002. Subcellular localization of the yeast proteome. *Genes Dev.* 16:707–719.

Leon, S., J.M. Goodman, and S. Subramani. 2006. Uniqueness of the mechanism of protein import into the peroxisome matrix: transport of folded, co-factor-bound and oligomeric proteins by shuttling receptors. *Biochim. Biophys. Acta.* 1763:1552–1564.

Liao, S.M., J. Zhang, D.A. Jeffery, A.J. Koleske, C.M. Thompson, D.M. Chao, M. Viljoen, H.J. van Vuuren, and R.A. Young. 1995. A kinase-cyclin pair in the RNA polymerase II holoenzyme. *Nature.* 374:193–196.

Marelli, M., J.J. Smith, S. Jung, E. Yi, A.I. Nesvizhskii, R.H. Christmas, R.A. Saleem, Y.Y. Tam, A. Fagarasanu, D.R. Goodlett, et al. 2004. Quantitative mass spectrometry reveals a role for the GTPase Rho1p in actin organization on the peroxisome membrane. *J. Cell Biol.* 167:1099–1112.

Navarro, B., and J.C. Igual. 1994. *ADR1* and *SNF1* mediate different mechanisms in transcriptional regulation of yeast *POT1* gene. *Biochem. Biophys. Res. Commun.* 202:960–966.

Pelkmans, L., E. Fava, H. Grabner, M. Hannus, B. Habermann, E. Krausz, and M. Zerial. 2005. Genome-wide analysis of human kinases in clathrin- and caveolae/raft-mediated endocytosis. *Nature.* 436:78–86.

Phelps, C., V. Gburcik, E. Suslova, P. Dudek, F. Forafonov, N. Bot, M. MacLean, R.J. Fagan, and D. Picard. 2006. Fungi and animals may share a common ancestor to nuclear receptors. *Proc. Natl. Acad. Sci. USA.* 103:7077–7081.

Platta, H.W., and R. Erdmann. 2007. The peroxisomal protein import machinery. *FEBS Lett.* 581:2811–2819.

Ptacek, J., G. Devgan, G. Michaud, H. Zhu, X. Zhu, J. Fasolo, H. Guo, G. Jona, A. Breitkreutz, R. Sopko, et al. 2005. Global analysis of protein phosphorylation in yeast. *Nature.* 438:679–684.

Rayapuram, N., and S. Subramani. 2006. The importomer—a peroxisomal membrane complex involved in protein translocation into the peroxisome matrix. *Biochim. Biophys. Acta.* 1763:1613–1619.

Roth, A.F., J. Wan, A.O. Bailey, B. Sun, J.A. Kuchar, W.N. Green, B.S. Phinney, J.R. Yates III, and N.G. Davis. 2006. Global analysis of protein palmitoylation in yeast. *Cell.* 125:1003–1013.

Rottensteiner, H., A.J. Kal, M. Filipits, M. Binder, B. Hamilton, H.F. Tabak, and H. Ruis. 1996. Pip2p: a transcriptional regulator of peroxisome proliferation in the yeast *Saccharomyces cerevisiae. EMBO J.* 15:2924–2934.

Rottensteiner, H., L. Wabnegger, R. Erdmann, B. Hamilton, H. Ruis, A. Hartig, and A. Gurvitz. 2003. *Saccharomyces cerevisiae PIP2* mediating oleic acid induction and peroxisome proliferation is regulated by Adr1p and Pip2p-Oaf1p. *J. Biol. Chem.* 278:27605–27611.

Saeed, A.I., V. Sharov, J. White, J. Li, W. Liang, N. Bhagabati, J. Braisted, M. Klapa, T. Currier, M. Thiagarajan, et al. 2003. TM4: a free, open-source system for microarray data management and analysis. *Biotechniques.* 34:374–378.

Saeed, A.I., N.K. Bhagabati, J.C. Braisted, W. Liang, V. Sharov, E.A. Howe, J. Li, M. Thiagarajan, J.A. White, and J. Quackenbush. 2006. TM4 microarray software suite. *Methods Enzymol.* 411:134–193.

Scholz, O., A. Thiel, W. Hillen, and M. Niederweis. 2000. Quantitative analysis of gene expression with an improved green fluorescent protein. *Eur. J. Biochem.* 267:1565–1570.

Shannon, P., A. Markiel, O. Ozier, N.S. Baliga, J.T. Wang, D. Ramage, N. Amin, B. Schwikowski, and T. Ideker. 2003. Cytoscape: a software environment for integrated models of biomolecular interaction networks. *Genome Res.* 13:2498–2504.

Simon, M., M. Binder, G. Adam, A. Hartig, and H. Ruis. 1992. Control of peroxisome proliferation in *Saccharomyces cerevisiae* by *ADR1*, *SNF1* (*CAT1*, *CCR1*) and *SNF4* (*CAT3*). *Yeast.* 8:303–309.

Smith, J.J., T.W. Brown, G.A. Eitzen, and R.A. Rachubinski. 2000. Regulation of peroxisome size and number by fatty acid β-oxidation in the yeast *Yarrowia lipolytica. J. Biol. Chem.* 275:20168–20178.

Smith, J.J., M. Marelli, R.H. Christmas, F.J. Vizeacoumar, D.J. Dilworth, T. Ideker, T. Galitski, K. Dimitrov, R.A. Rachubinski, and J.D. Aitchison. 2002. Transcriptome profiling to identify genes involved in peroxisome assembly and function. *J. Cell Biol.* 158:259–271.

Smith, J.J., Y. Sydorskyy, M. Marelli, D. Hwang, H. Bolouri, R.A. Rachubinski, and J.D. Aitchison. 2006. Expression and functional profiling reveal distinct gene classes involved in fatty acid metabolism. *Mol. Syst. Biol.* 2:2006.

Smith, J.J., S.A. Ramsey, M. Marelli, B. Marzolf, D. Hwang, R.A. Saleem, R.A. Rachubinski, and J.D. Aitchison. 2007. Transcriptional responses to fatty acid are coordinated by combinatorial control. *Mol. Syst. Biol.* 3:115.

Strahl, T., and J. Thorner. 2007. Synthesis and function of membrane phosphoinositides in budding yeast, *Saccharomyces cerevisiae. Biochim. Biophys. Acta.* 1771:353–404.

Tam, Y.Y.C., A. Fagarasanu, M. Fagarasanu, and R.A. Rachubinski. 2005. Pex3p initiates the formation of a preperoxisomal compartment from a subdomain of the endoplasmic reticulum in *Saccharomyces cerevisiae. J. Biol. Chem.* 280:34933–34939.

van Roermund, C.W.T., H.F. Tabak, M. van Den Berg, R.J.A. Wanders, and E.H. Hettema. 2000. Pex11p plays a primary role in medium-chain fatty acid oxidation, a process that affects peroxisome number and size in *Saccharomyces cerevisiae. J. Cell Biol.* 150:489–498.

Voronkova, V., N. Kacherovsky, C. Tachibana, D. Yu, and E.T. Young. 2006. Snf1-dependent and Snf1-independent pathways of constitutive *ADH2* expression in *Saccharomyces cerevisiae. Genetics.* 172:2123–2138.

Zhu, H., J.F. Klemic, S. Chang, P. Bertone, A. Casamayor, K.G. Klemic, D. Smith, M. Gerstein, M.A. Reed, and M. Snyder. 2000. Analysis of yeast protein kinases using protein chips. *Nat. Genet.* 26:283–289.